Applied and Computational Mathematics
2026; 15(1): 13-25
http://www.sciencepublishinggroup.com/j/acm
doi: 10.11648/j.acm.20261501.12

Investigating the Effects of Joule Heating on Chemically Reactive Williamson Fluid over an Inclined Rotating Surface

Tabitha Kerubo Ong'au[1, *], Johanna Kibet Sigey[1], Viona Nakhulo Ojiambo[1], Moffat Chamuchi[2]

[1]Department of Pure and Applied Mathematics, Jomo Kenyatta University of Agriculture and Technology, Juja, Kenya
[2]Department of Pure and Applied Mathematics, Kirinyaga University, Kerugoya, Kenya

Email address:
kerubotabitha@yahoo.com (Tabitha Kerubo Ong'au)
[*]Corresponding author

To cite this article:
Tabitha Kerubo Ong'au, Johanna Kibet Sigey, Viona Nakhulo Ojiambo, Moffat Chamuchi. (2026). Investigating the Effects of Joule Heating on Chemically Reactive Williamson Fluid over an Inclined Rotating Surface. *A*pplied and Computational Mathematics, 15(1), 13-25. https://doi.org/10.11648/j.acm.20261501.12

Received: 30 September 2025; **Accepted:** 7 November 2025; **Published:** 15 January 2026

Abstract: This study focuses on the analysis of the flow behaviour of a chemically reacting Williamson fluid over an inclined rotating surface, taking into account the combined effects of Coriolis force and Joule heating. A mathematical model is developed to describe the fluid dynamics by integrating the equations of momentum, energy, and species concentration under the influence of these physical phenomena. The governing partial differential equations have been non-dimensionalised and transformed into a system of ordinary differential equations by introducing similarity transform. The resulting ODEs are written as a truncated series whose coefficients are obtained by using the collocation numerical technique on the resulting equations. The flow variables are determined and presented in profile and tabular form. The results were validated by comparing with MATLAB bvp4c and the error ranges between 0.09% and 0.61%, indicating that the method of solution is admissible. It is established that the Coriolis force enhances fluid velocity while simultaneously reducing both temperature and concentration. In contrast, Joule heating increases temperature but decreases fluid velocity and concentration. Additionally, chemical reactions lead to a reduction in velocity and concentration due to the consumption of reactive species, while simultaneously increasing temperature due to exothermic effects.

Keywords: Joule Heating, Chemical Reaction, Williamson Fluid, Inclined Surface, Coriolis Force

1. Background of the Study

Fluids are broadly classified as Newtonian and non-Newtonian fluids [1]. However, the non-Newtonian fluids are more common in nature [2]. The frequent use of non-Newtonian fluids in nature necessitated the need to develop models that can be used investigate the behaviours [3, 4]. Eyring-Powell fluid [5], Carreau fluid [6], Casson fluid [7], and Williamson fluid [8] are examples of non-Newtonian fluids. Ouru et al. [9] examined the Williamson fluid, Leelavathi et al. [7] and Oke et al. [10] investigated the Casson fluid, Vyakaranam et al. [11] discussed Walters-B fluid, Oke et al. [12] introduced the Modified Eyring Powell fluid, and Rutto et al. [13] investigated water-based nanofluid. However, Williamson fluid models fluids whose viscosity decreases with increasing shear rates [14]. Studies by Khan et al. [15], Ouru et al. [9], and Juma et al. [16] have explored the behaviour of MHD Williamson fluids over rotating and stretching surfaces. Their work demonstrated that as the rotation rate increased, so did the fluid velocity. This suggests that the response of the Williamson fluid to rotation could enhance its motion. Yusuf and Mabood [17] examined how chemical reactions influence magnetohydrodynamic (MHD) Williamson fluids, particularly when flowing over an inclined permeable wall. Srinivasulu and Goud [18] delved into how Lorentz forces affect the flow of Williamson nanofluids. Meanwhile, Li et al. [19] focused on heat generation and absorption in Williamson nanofluids under MHD conditions, showing that thermal processes play a significant role in altering fluid behaviour.

Joule heating occurs when an electric current passes through a conductive fluid, resulting in the dissipation of electrical energy into heat [20]. This phenomenon is common in systems where fluids conduct electricity, such as electrolytes, molten metals, and plasma. The heat generated due to Joule heating increases the temperature of the fluid, which can, in turn, affect its viscosity and other physical properties. In systems where both heat transfer and fluid flow are important, Joule heating can have a significant impact. For instance, in electrically heated reactors or furnaces [21], the heat generated by the current flow must be carefully controlled to ensure the desired temperature distribution within the fluid. In fluid flow systems, where both thermal and electrical energy are involved, the interaction between Joule heating and the fluid's physical properties can influence the overall flow behaviour. In this study, Joule heating is an important factor as it affects the temperature profile of the Williamson fluid and, consequently, its flow characteristics.

Rotating surfaces experiences the Coriolis forces that significantly affect fluid motion [22, 23]. Coriolis force is an apparent force that acts on objects moving within a rotating reference frame. It arises due to the rotation of the surface and affects the direction of moving objects [1]. Rotating surfaces are important in rotating reactors and mechanical systems where fluid is transported over rotating surfaces [16, 24, 25]. Oke [1] provided insight into the effects of Coriolis force on different types of fluid over a non-uniform surface. Oke et al.[24] investigated how MHD flows behave on rotating, non-uniform surfaces and found that increasing the rotation rate enhances heat transfer by pushing the fluid outwards. Similarly, when analysing non-Newtonian fluids, Oke et al. [26] and Oke et al. [2] demonstrated that both velocity and temperature profiles increase with greater rotational speed. Similarly, Oke [27] showed that the Coriolis force reduces skin friction but enhances heat transfer in ternary hybrid nanofluids under MHD conditions. Oke et al. [12] found that increasing the Coriolis force leads to a drop in velocity while raising the temperature, as the force diverts the flow away from the axis of rotation. Alhefthi et al. [3] studied how thermal radiation affects MHD nanofluid flows in confined geometries, focusing on squeezing effects and thermophoresis. These factors lead to changes in heat transfer rates and the movement of nanoparticles within the fluid. Areekara et al. [28] explored Darcy-Forchheimer flow over rotating discs, showing how magnetic fields interact with the porous medium to alter heat transfer rates. Ali et al. [25] examined the thermodynamics of rotating dusty Maxwell-TiO2 and dust particles nanofluids. They found that these additional factors alter both the flow and heat transfer properties of the fluid. Alsaud et al. [4] investigated the response of velocity and temperature profiles to the reactive MHD couple stress fluids.

Despite the extensive research on fluid flow over inclined and rotating surfaces, significant gaps remain in understanding the combined effects of chemical reactions and Joule heating on Williamson fluids. Previous studies have explored MHD flows and the impact of Coriolis forces on non-Newtonian fluids [1, 5, 12, 14]. However, these studies often neglect the comprehensive interaction between thermal and solutal buoyancy forces, chemical reactions, and thermophoretic effects under rotating conditions. This study investigates a steady boundary layer flow of a viscous, thermally and electrically conducting Williamson fluid over a rotating inclined porous plate.

2. The Model Formulation

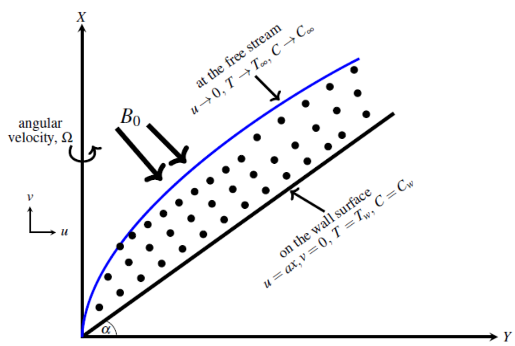

Figure 1. Flow configuration.

Consider a linearly stretching inclined surface rotating at a constant angular velocity Ω positioned at an angle α to the horizontal, as depicted in Figure (1). A uniform magnetic field of strength B_0 is applied perpendicularly to the flow, oriented at $\frac{\pi}{2}$rad to the flow direction. The conditions at the wall are dictated by the no-slip condition so that $u = ax$, (where a is a constant) at the wall. The equation governing the flow of chemically reacting Williamson fluid over an inclined rotating surface with Joule heating is the coupled partial differential equation.

$$\frac{\partial u}{\partial x}+\frac{\partial v}{\partial y} =0, \tag{1}$$

$$u\frac{\partial u}{\partial x}+v\frac{\partial u}{\partial y} =\vartheta\left(1+\frac{2\Gamma}{\sqrt{2}}\frac{\partial u}{\partial y}\right)\frac{\partial^2 u}{\partial y^2}+g\left(\beta\left(T-T_\infty\right)+\beta^*\left(C-C_\infty\right)\right)\cos\alpha+2\Omega u-\frac{\sigma B_0^2 u}{\rho}-\frac{\nu}{\rho}u, \tag{2}$$

$$u\frac{\partial T}{\partial x}+v\frac{\partial T}{\partial y} =\frac{\kappa}{\rho c_p}\frac{\partial^2 T}{\partial y^2}+\tau\left(\frac{D_B}{\Delta C}\frac{\partial C}{\partial y}\frac{\partial T}{\partial y}+\frac{D_T}{T_\infty}\left(\frac{\partial T}{\partial y}\right)^2\right)-\frac{\sigma B^2}{(\rho C_p)}u^2, \tag{3}$$

$$u\frac{\partial C}{\partial x}+v\frac{\partial C}{\partial y} =D_B\frac{\partial^2 C}{\partial y^2}+\frac{D_T\Delta C}{T_\infty}\frac{\partial^2 T}{\partial y^2}-\frac{K_c}{(\rho C_p)}\left(C-C_\infty\right). \tag{4}$$

with the boundary conditions

$$\begin{cases} u=ax,\ v=0,\ T=T_w,\ C=C_w,\ \text{at}\ y=0,\\ u\to 0,\ T\to T_\infty,\ C\to C_\infty,\ \text{as}\ y\to\infty. \end{cases} \tag{5}$$

The skin drag, heat transfer rate and mass transfer rate defined are defined following the definition of Sheri and Modugula [29] as

$$C_f=-\frac{2\vartheta}{a^2}\left(u_y+\frac{\sqrt{2}\Gamma}{2}u_y^2\right)_{y=0},\ Nu=-\frac{xT_y\left(x,0\right)}{\left(T_w-T_\infty\right)},\ Sh=-\frac{xC_y\left(x,0\right)}{\left(C_w-C_\infty\right)} \tag{6}$$

3. Similarity Transformation

For the equation under consideration, the appropriate similarity variables are

$$\eta=y\left(\frac{a}{\vartheta}\right)^{\frac{1}{2}},\ u=ax\frac{df}{d\eta},\ v=-\left(a\vartheta\right)^{\frac{1}{2}}f.. \tag{7}$$

and the temperature and concentration can be rescaled as

$$T=\left(T_w-T_\infty\right)\theta+T_\infty,\ C=\left(C_w-C_\infty\right)\Phi+C_\infty. \tag{8}$$

The dimensionless equations become;

$$\left(1+\gamma\frac{d^2 f}{d\eta^2}\right)\frac{d^3 f}{d\eta^3}-\left(\frac{df}{d\eta}\right)^2+f\frac{d^2 f}{d\eta^2}+\left(K-M-s\right)\frac{df}{d\eta}+\left(Gr_t\theta+Gr_s\Phi\right)\cos\alpha=0. \tag{9}$$

$$\frac{d^2\theta}{d\eta^2}+Prf\frac{d\theta}{d\eta}+N_b\frac{d\theta}{d\eta}\frac{d\Phi}{d\eta}+N_t\left(\frac{d\theta}{d\eta}\right)^2-MJPr\left(\frac{df}{d\eta}\right)^2=0 \tag{10}$$

$$\frac{d^2\Phi}{d\eta^2}+Scf\frac{d\Phi}{d\eta}+\frac{N_t}{N_b}\frac{d^2\theta}{d\eta^2}-rSc\Phi=0. \tag{11}$$

with the condition

$$\frac{df}{d\eta}=1,\ f=0,\ \theta=1,\ \Phi=1 \text{ when } \eta=0, \tag{12}$$

$$\frac{df}{d\eta}\to 0,\ \theta\to 0,\ \Phi\to 0 \text{ when } \eta\to\infty. \tag{13}$$

and define the parameters as

$$\gamma=\sqrt{2}ax\Gamma\left(\frac{a}{\vartheta}\right)^{\frac{1}{2}},\ K=\frac{2\Omega}{a},\ M=\frac{\sigma B_0^2}{\rho a},\ s=\frac{\nu}{a\rho},\ Re^{-\frac{1}{2}}=x\left(\frac{\vartheta}{a}\right)^{\frac{1}{2}},\ Gr_t=\frac{g}{a^2x}\beta\left(T_w-T_\infty\right),$$
$$Gr_s=\frac{g}{a^2x}\beta^*\left(C_w-C_\infty\right),Pr=\frac{\vartheta}{\alpha}=\frac{\rho c_p\vartheta}{\kappa},\ N_b=\frac{\tau D_B}{\alpha},\ N_t=\frac{\tau D_T\left(T_w-T_\infty\right)}{\alpha T_\infty},\ M=\frac{\sigma B_0^2}{\rho a x},$$
$$J=\frac{a^2x}{C_p\left(T_w-T_\infty\right)},\ Sc=\frac{\vartheta}{D_B},\ r=\frac{K_c}{a\left(\rho C_p\right)}.$$

The engineering quantities become:

$$Re^{\frac{1}{2}}C_f=-\left(\frac{d^2f}{d\eta^2}+\frac{\lambda}{2}\left(\frac{d^2f}{d\eta^2}\right)^2\right)_{\eta=0},\ .\ Re^{-\frac{1}{2}}Nu=-\left(\frac{d\theta}{d\eta}\right)_{\eta=0},\ Re^{-\frac{1}{2}}Sh=-\left(\frac{d\Phi}{d\eta}\right)_{\eta=0}. \tag{14}$$

By setting

$$f=g_1,f'=g_2,f''=g_3,\theta=g_4,\theta'=g_5,\Phi=g_6,\Phi'=g_7, \tag{15}$$

then equations (9 - 11) are reformulated as a first-order system;

$$\begin{cases} g_1'=g_2,\ g_2'=g_3,\\ g_3'=-\frac{-g_2^2+g_1g_3+(K-M-s)g_2+(Gr_tg_4+Gr_sg_6)\cos\alpha}{1+\gamma g_3},\\ g_4'=g_5,\ g_5'=-\left(Prg_1g_5+N_bg_5g_7+N_tg_5^2-M\cdot J\cdot Pr\cdot g_2^2\right),\\ g_6'=g_7,\ g_7'=-\left(Scg_1g_7+\frac{N_t}{N_b}g_5'-rScg_6\right). \end{cases} \tag{16}$$

with the conditions

$$g_2=1,\ g_1=0,\ g_4=1,\ g_6=1 \text{ when } \eta=0, \tag{17}$$

$$g_2\to 0,\ g_4\to 0,\ g_6\to 0 \text{ when } \eta\to\eta_\infty. \tag{18}$$

4. Collocation Technique

Given a system of equations

$$g'=f\left(g_1,g_2,\cdots,g_n\right),\ g=\left(g_1\left(\eta\right),g_2\left(\eta\right),\cdots,g_n\left(\eta\right)\right),\ g\left(0\right)=a,g\left(\eta_\infty\right)=b.$$

Start by approximating $g_i\left(\eta\right)$ [30] as a linear combination of the basis functions $\phi_j\left(\eta\right)$ and unknown coefficients $c_{i,j}$

$$g_i\left(\eta\right)\approx S\left(\eta\right)=\sum_{j=0}^{N}c_{i,j}\phi_j\left(\eta\right),$$

Thus,

$$g_i'(\eta) \approx S'(\eta) = \sum_{j=0}^{N} c_{i,j}\phi_j'(\eta)$$
$$\mathcal{R}(\eta) = S'(\eta) - f = \sum_{j=0}^{N} c_{i,j}\phi_j'(\eta) - f.$$

where $\mathcal{R}(\eta)$ is the residual and $c_{i,j}$ are unknowns to be obtained by minimising $\mathcal{R}(\eta)$. Write the residuals for the system (16) as

$$\mathcal{R}_j = g_j' - g_{j+1},\ j = 1,2,4,6 \tag{19}$$
$$\mathcal{R}_3 = (1+\gamma g_3)\,g_3' - g_2^2 + g_1 g_3 + (K - M - s)\,g_2 + (Gr_t g_4 + Gr_s g_6)\cos\alpha, \tag{20}$$
$$\mathcal{R}_5 = g_5' + Pr g_1 g_5 + N_b g_5 g_7 + N_t g_5^2 - M\cdot J\cdot Pr\cdot g_2^2, \tag{21}$$
$$\mathcal{R}_7 = g_7' + Sc g_1 g_7 + \frac{N_t}{N_b} g_5' - rSc g_6. \tag{22}$$

with the accompanying conditions;

$$g_1(0) = 0,\ g_2(0) = 1,\ g_4(0) = 1,\ g_6(0) = 1, \tag{23}$$
$$g_2(\infty) = 0,\ g_4(\infty) = 0,\ \Phi(\infty) = 0. \tag{24}$$

The collocation method is adopted in solving the system of equations (19 - 22). Subdivide the domain by choosing an $N+1$ collocation points $\eta_k\ (k = 0,1,\cdots,N) \in [0,\eta_\infty]$ and let basis functions be piecewise cubic polynomials, then

$$g_i \approx a_{ik} + b_{ik}\xi_k + c_{ik}\xi_k^2 + d_{ik}\xi_k^3,\ i = 1,2,\cdots,7,\ \xi_k = \eta - \eta_k \tag{25}$$
$$g_i' \approx b_{ik} + 2c_{ik}\xi_k + 3d_{ik}\xi_k^2,\ i = 1,2,\cdots,7 \tag{26}$$

Coefficients are determined by minimising the residuals at selected collocation points in each subinterval. By putting (25) and (26) into equation (19), we have

$$-a_{2k} + b_{1k} = 0,\ 2c_{1k} - b_{2k} = 0,\ 3d_{1k} - c_{2k} = 0,\ d_{2k} = 0. \tag{27}$$
$$-a_{3k} + b_{2k} = 0,\ 2c_{2k} - b_{3k} = 0,\ 3d_{2k} - c_{3k} = 0,\ d_{3k} = 0. \tag{28}$$
$$-a_{5k} + b_{4k} = 0,\ 2c_{4k} - b_{5k} = 0,\ 3d_{4k} - c_{5k} = 0,\ d_{5k} = 0. \tag{29}$$
$$-a_{7k} + b_{6k} = 0,\ 2c_{6k} - b_{7k} = 0,\ 3d_{6k} - c_{7k} = 0,\ d_{7k} = 0. \tag{30}$$

By putting (25) and (26) into equation (20), comparing coefficients, and substituting $d_{jk} = 0, (j = 2,3,5,7)$, then $c_{3k}d_{1k} = 0$ and

$$\begin{aligned}&3\gamma b_{3k}c_{3k} - 2a_{2k}c_{2k} - b_{2k}^2 + a_{1k}c_{3k} + b_{1k}b_{3k} + a_{3k}c_{1k} + (K - M - s)\,c_{2k}\\&\quad + (Gr_t c_{4k} + Gr_s c_{6k})\cos\alpha = 0\end{aligned} \tag{31}$$
$$2\gamma c_{3k}^2 - 2b_{2k}c_{2k} + b_{1k}c_{3k} + b_{3k}c_{1k} + a_{3k}d_{1k} + (Gr_t d_{4k} + Gr_s d_{6k})\cos\alpha = 0 \tag{32}$$
$$-c_{2k}^2 + c_{1k}c_{3k} + b_{3k}d_{1k} = 0 \tag{33}$$

By putting (25) and (26) into equation (21), compiling the coefficients and substituting $d_{jk} = 0, (j = 2,3,5,7)$, then

$Prc_{5k}d_{1k} + N_b c_{5k} d_{7k} = 0$ and

$$Pr\left(a_{1k}c_{5k} + b_{1k}b_{5k} + a_{5k}c_{1k}\right) + N_b\left(a_{5k}c_{7k} + b_{5k}b_{7k} + a_{7k}c_{5k}\right) + N_t\left(2a_{5k}c_{5k} + b_{5k}^2\right) - MJPr\left(2a_{2k}c_{2k} + b_{2k}^2\right) = 0, \tag{34}$$

$$Pr\left(b_{1k}c_{5k} + b_{5k}c_{1k} + a_{5k}d_{1k}\right) + N_b\left(a_{5k}d_{7k} + b_{5k}c_{7k} + b_{7k}c_{5k}\right) + 2N_t b_{5k}c_{5k} - 2MJPrb_{2k}c_{2k} = 0, \tag{35}$$

$$Pr\left(c_{1k}c_{5k} + b_{5k}d_{1k}\right) + N_b\left(b_{5k}d_{7k} + c_{5k}c_{7k}\right) + N_t c_{5k}^2 - MJPrc_{2k}^2 = 0. \tag{36}$$

By putting (25) and (26) into equation (22), compiling the coefficients, and substituting $d_{jk} = 0, (j = 2, 3, 5, 7)$, then $Scd_{1k}c_{7k} = 0$ and

$$-rScc_{6k} + Sca_{7k}c_{1k} + Scb_{1k}b_{7k} + Sca_{1k}c_{7k} = 0 \tag{37}$$

$$-rScd_{6k} + Sca_{7k}d_{1k} + Scb_{7k}c_{1k} + Scb_{1k}c_{7k} = 0 \tag{38}$$

$$Scb_{7k}d_{1k} + Scc_{1k}c_{7k} = 0 \tag{39}$$

Hence, we set $d_{jk} = 0, (j = 2, 3, 5, 7)$, and solve the system of equations over the interval $\left(\eta_k, \eta_{k+1}\right)$ using the Newton's method with the global boundary conditions:

$$\begin{cases} g_1\left(0\right) = a_{1k} - \eta_k b_{1k} + c_{1k}\eta_k^2 - d_{1k}\eta_k^3 = 0, \\ g_i\left(0\right) = a_{ik} + b_{ik}\eta_k + c_{ik}\eta_k^2 + d_{ik}\eta_k^3 = 1, \ i = 2, 4, 6 \\ g_i\left(\eta_\infty\right) = a_{ik} + b_{ik}\left(\eta_\infty - \eta_k\right) + c_{ik}\left(\eta_\infty - \eta_k\right)^2 - d_{ik}\left(\eta_\infty - \eta_k\right)^3 = 0, \ i = 2, 4, 6 \end{cases} \tag{40}$$

5. Validation of Results

To analyse stability, the eigenvalues of the Jacobian matrix were computed for varying values of the parameters. Results are reported in Table (1). Since all eigenvalues are non-positive, the numerical method is stable for $r \in [0.01, 1.6]$. The results is validated by comparing the present result with the work of Ahmed and Akbar [31] and Juma et al. [16] by setting

$$K = M = s = Gr_t = Gr_s = Pr = N_t = J = Sc = r = \alpha = 0.$$

Table (2) validates the numerical method adopted in this study since the present results in good agreement with the existing literature.Subsequently, the solution is simulated for various values of the emerging parameters over the interval $\eta \in [0, 20]$.

Table 1. *Stability Analysis of the Method by varying r.*

r	**Eigenvalues**						
0.001	-1.5763	-1.7837	-0.2536	-0.2536	0.000	-0.4806	-0.4806
0.4	-1.5914	-1.7966	-0.4174	-0.4174	0.000	-0.6456	-0.6456
0.8	-1.6083	-1.8108	-0.5146	-0.5146	0.000	-0.7442	-0.7442
1.2	-1.6274	-1.8264	-0.5871	-0.5871	0.000	-0.8184	-0.8184
1.6	-1.8436	-0.8788	-0.8788	0.0000	-0.6455	-0.6455	-1.6487

Table 2. *Comparison of results with existing literature.*

γ	**0.0000**	**0.1000**	**0.2000**	**0.3000**
Ahmed and Akbar [31]	1.3393	1.2980	1.2631	1.2228
Juma et al. [16]	1.3301	1.2988	1.2638	1.2235
Present study	1.3381	1.3057	1.2714	1.2344

6. Results and Discussion

Solutions to the system of equations are obtained for various values of reactiveness r, Joule heating J, Coriolis force, and angle of inclination α. Default values for the parameters are

$$\begin{aligned} \gamma = 0.1; K = 0.1; M = 2; s = 0.2; \\ Gr_t = 1; Gr_s = 1; \alpha = \frac{\pi}{6}; \\ Pr = 4; N_b = 0.1; N_t = 0.1; \\ J = 0.25; Sc = 0.62; r = 0.4. \end{aligned}$$

The impact of reactiveness on the behaviour of the fluid is observed through its influence on velocity, temperature, and concentration profiles. The primary and secondary velocity profiles, illustrated in Figures (2a) and (2b), exhibit a clear decreasing trend with increasing reactiveness. This behaviour indicates that chemical reactions within the fluid medium introduce resistance to motion, a phenomenon that can be interpreted as a dissipative mechanism. As reactiveness increases, the energy required to sustain fluid motion is partially consumed by chemical processes. This energy diversion reduces the kinetic energy available for the fluid flow, thereby lowering both primary and secondary velocities. This finding is consistent with theoretical principles, where chemical activity, especially in reactive flows, contributes to momentum dissipation. The temperature profile, depicted in Figure (3a), reveals an increasing trend with higher reactiveness. This rise in temperature is attributable to the exothermic nature of chemical reactions occurring within the fluid. In exothermic reactions, the release of thermal energy not only elevates the temperature of the immediate reaction zone but also contributes to the overall thermal energy within the system. Figure (3b) shows that concentration decreases with reactiveness. The concentration of reactive species decreases due to their consumption in chemical reactions. This depletion demonstrates the effectiveness of the reactive processes in altering the chemical composition of the fluid.

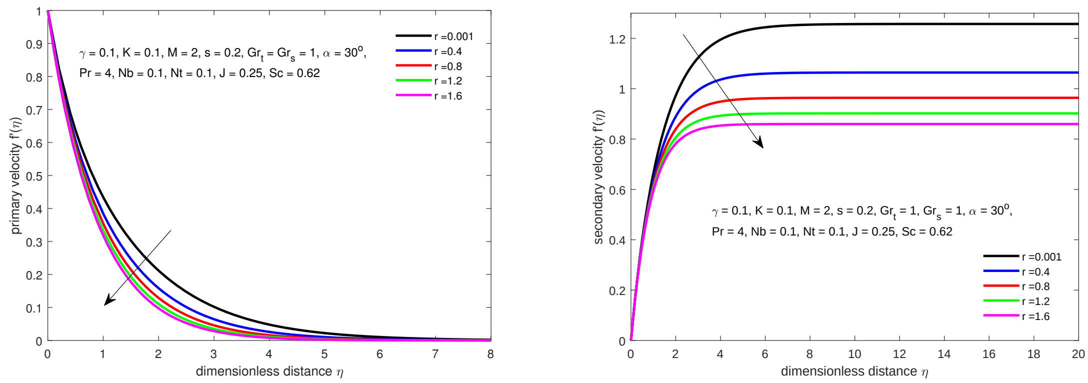

(a) Effect of reactiveness on primary velocity **(b)** Effect of reactiveness on secondary velocity

Figure 2. *Effect of reactiveness on velocity.*

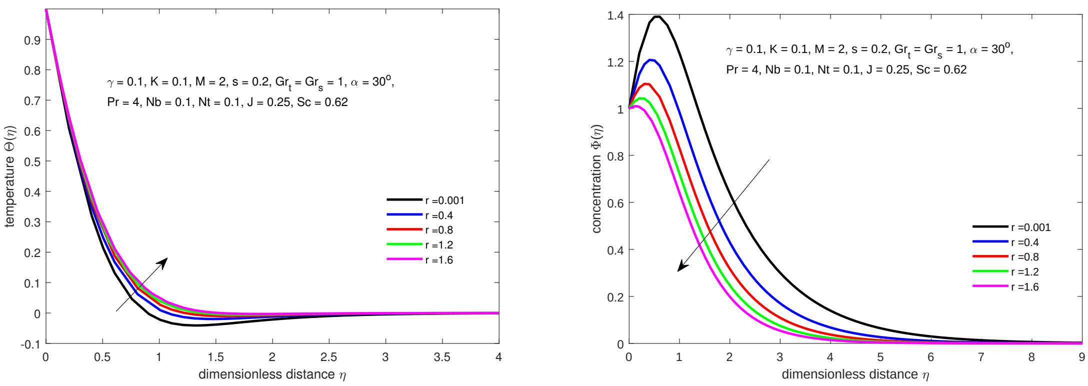

(a) Effect of reactiveness on temperature **(b)** Effect of reactiveness on concentration

Figure 3. *Effect of reactiveness on temperature and concentration.*

The effects of Joule heating on velocity, temperature, and concentration profiles are studied in this section. Figures (4a) and (4b) show that both primary and secondary velocities exhibit a decline under the influence of Joule heating. This reduction can be associated to the increased viscous effects caused by the heat generated from electrical energy dissipation. From Figure (5a), the temperature response to Joule heating is increasing. As Joule heating persists, the accumulation of thermal energy becomes dominant, leading to an increase in temperature. The observations in Figure (5b), shows that concentration exhibits a decreasing trend with increasing Joule Heating. This pattern could result from a diffusion-dominated regime transitioning into one where thermal gradients enhance solute transport.

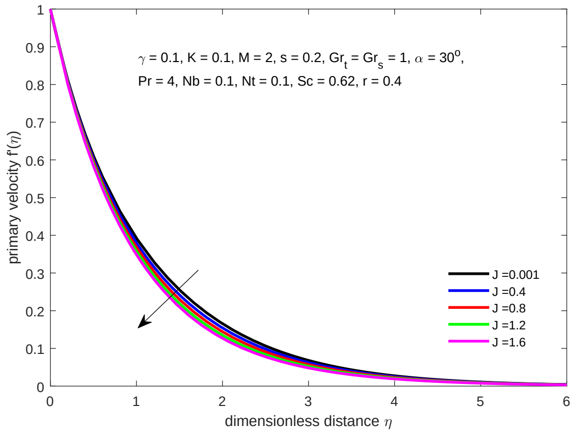

(a) Effect of Joule heating on primary velocity

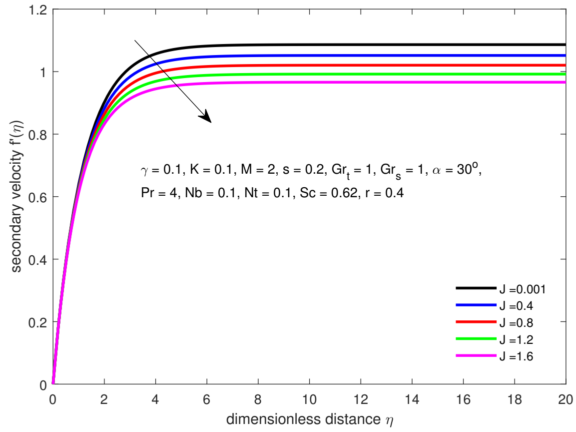

(b) Effect of Joule heating on secondary velocity

Figure 4. *Effect of Joule heating on velocity.*

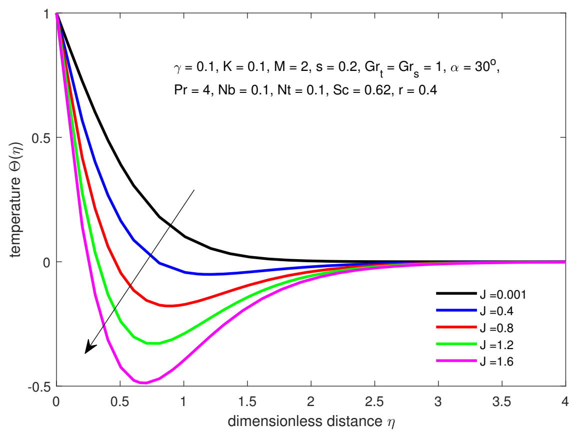

(a) Effect of Joule heating on temperature

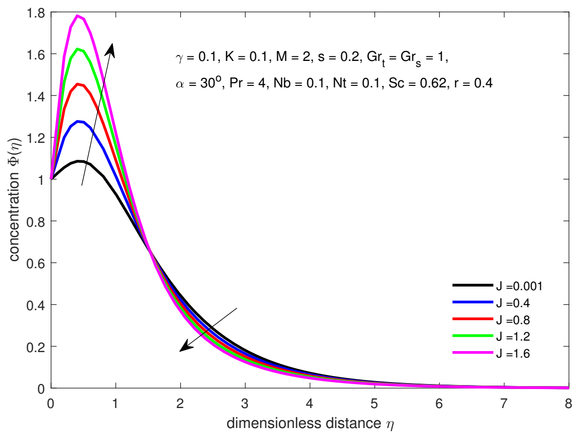

(b) Effect of Joule heating on concentration

Figure 5. *Effect of Joule heating on temperature and concentration.*

The influence of the Coriolis force, arising from the rotational motion of the reference frame, on the fluid flow is discussed hereby. Figure (6a) and (6b) shows that both primary and secondary velocities increase with a stronger Coriolis effect. This enhancement can be attributed to the rotational forces imparting additional energy into the system, which accelerates fluid motion in both directions. This finding is particularly relevant in geophysical and astrophysical contexts, where Coriolis forces play a critical role in shaping flow patterns. In contrast, Figure (7a) shows that the temperature profile decreases with increasing Coriolis force. The augmented motion facilitated by the rotational forces enhances convective heat transfer, thereby dissipating thermal energy from the system more efficiently.

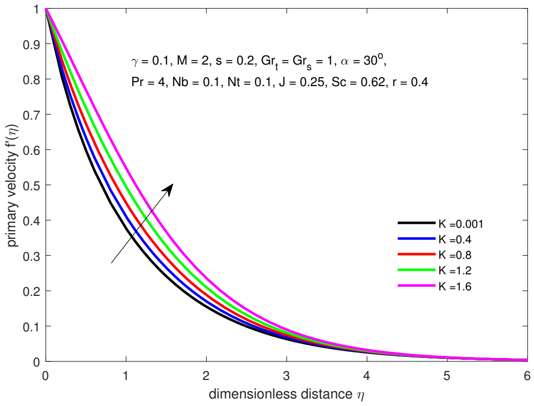

(a) Effect of Coriolis force on primary velocity

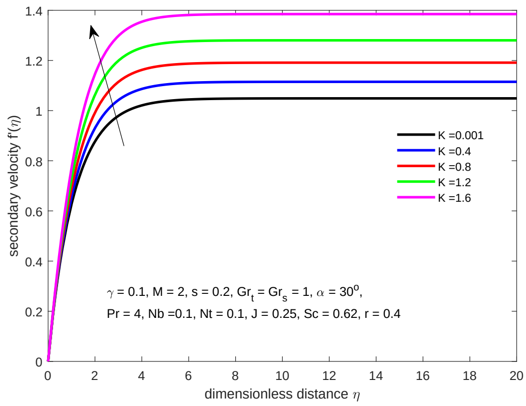

(b) Effect of Coriolis force on secondary velocity

Figure 6. *Effect of Coriolis force on velocity.*

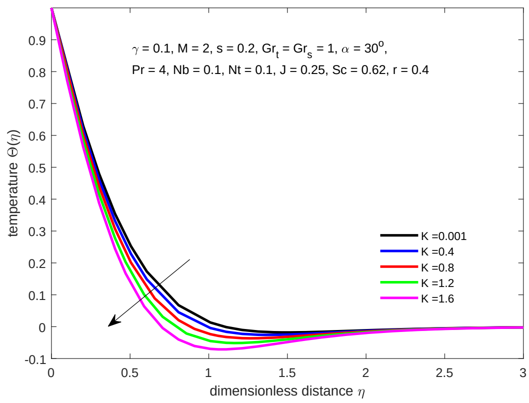

(a) Effect of Coriolis force on temperature

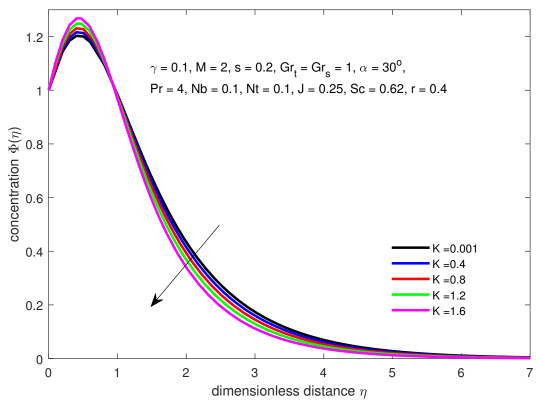

(b) Effect of Coriolis force on concentration

Figure 7. *Effect of Coriolis force on temperature and concentration.*

6.1. Engineering Quantities of Interest

The quantities of engineering interest are reported in Table (3). Table (3) reveals that as Joule heating and Coriolis force increase, the skin friction and Nusselt number tend to rise, suggesting that higher energy dissipation and stronger Coriolis effects lead to increased resistance to flow and enhanced heat transfer. The reactiveness parameter remains largely constant, which indicates that changes in the energy dynamics have a more significant impact on skin friction and heat transfer rate than on the reactivity of the system itself. The angle of inclination also seems to play a relatively minor role in influencing the results, with only a few entries showing variations in its effect on the system. The Sherwood number increases with increasing Joule heating and Coriolis force while it decreases with reactiveness and and angle of inclination.

Table 3. *Variations in the quantities of interest with the parameters.*

J	k	r	$alpha$	Skin Friction $Re^{1/2}Cf$	Nusselt number $Re^{-1/2}Nu$	Sherwood number $Re^{-1/2}Sh$
0.5	0.1	0.4	$\frac{\pi}{6}$	2.054267863	2.704889604	1.513285072
0.8	0.1	0.4	$\frac{\pi}{6}$	2.074370684	3.452953567	2.212182853
1.1	0.1	0.4	$\frac{\pi}{6}$	2.093130501	4.171717755	2.884794094
0.25	0.5	0.4	$\frac{\pi}{6}$	1.759659427	2.127934995	0.957456635
0.25	0.8	0.4	$\frac{\pi}{6}$	1.53749399	2.187824688	0.99828013
0.25	1.1	0.4	$\frac{\pi}{6}$	1.300856598	2.253943499	1.043096655

J	k	r	$alpha$	Skin Friction $Re^{1/2}Cf$	Nusselt number $Re^{-1/2}Nu$	Sherwood number $Re^{-1/2}Sh$
0.25	0.1	0.5	$\frac{\pi}{6}$	2.058703763	2.041623272	0.818850405
0.25	0.1	0.8	$\frac{\pi}{6}$	2.114321336	2.006225271	0.588113572
0.25	0.1	1.1	$\frac{\pi}{6}$	2.158043932	1.979570285	0.396985404
0.25	0.1	0.4	0	1.836138907	2.110367612	0.945237229
0.25	0.1	0.4	$\frac{\pi}{13}$	1.879351764	2.098798117	0.937325537
0.25	0.1	0.4	$\frac{4\pi}{13}$	2.491339773	1.928762692	0.821878922
0.25	0.1	0.4	$\frac{6\pi}{13}$	3.206709941	1.712988742	0.677951076

7. Conclusion

A chemically reacting Williamson fluid over an inclined rotating surface, considering the influences of Coriolis force and Joule heating has been studied. The investigation attempts to understand how these physical phenomena impact the velocity, temperature, and concentration profiles within the fluid system. The objectives of this study were successfully achieved, and the research made significant contributions to understanding the behaviour of Williamson fluids subjected to Coriolis force, Joule heating, and chemical reactions over an inclined rotating surface. The results were validated by comparing with MATLAB bvp4c and the error ranges between 0.09% and 0.61%, indicating that the method of solution is admissible. The influence of angle of inclination, Coriolis force, Joule heating, and chemical reaction on the velocity, temperature, and concentration profiles was analysed. It is found that the Coriolis force enhances the velocity of the fluid while reducing the temperature and concentration. Joule heating increases the temperature but reduces the velocities and concentration due to enhanced viscous effects. Chemical reactivity reduces the velocity profiles but increases the temperature due to the exothermic nature of the reactions, while the concentration decreases as reactive species are consumed. Joule heating and Coriolis force rise, they significantly increase skin friction, heat transfer rate, and mass transfer rate, while the reactiveness parameter and angle of inclination exert only minor effects on the system.

ORCID

0009-0004-1790-7351 (Johanna Kibet Sigey)
0000-0002-3311-5539 (Viona Nakhulo Ojiambo)
0009-0001-3150-2404 (Moffat Chamuchi)

Abbreviations

F_c	Coriolis Force
J	Joule Heating Parameter
B_0	Magnetic Field Strength
Sc	SCHMIDT Number
u, v	Vertical and Horizontal Velocity
Gr_t, Gr_s	Thermal and Solutal Grashof Number
T, C	Temperature, Concentration Respectively
N_b, N_t	Brownian and Thermophoretic Parameters Respectively
g	Acceleration Due to Gravity
Nu	Nusselt Number
K	Coriolis Force Parameter
Sh	Sherwood Number
M	Magnetic Field Parameter
f'	Dimensionless Velocity
s	Porosity Parameter
C_f	Skin Friction
Pr	Prandtl Number
r	Chemical Reaction Parameter
τ	Shear Stress
ρ	Density
Ω	Angular Velocity
η	Similarity Variable
α	Angle of Inclination
γ	Williamson Fluid Parameter
μ	Dynamic Viscosity
θ	Dimensionless Temperature
ϑ	Kinematic Viscosity
Φ	Dimensionless Concentration

Conflicts of Interest

The authors declare no conflicts of interest.

References

[1] Abayomi Samuel Oke. Coriolis Effects on Air, Nanofluid and Casson Fluid Flow over a Surface with non-Uniform Thickness. PhD thesis, Kenyatta University, 2022.

[2] A. S. Oke, I. L. Animasaun, W. N. Mutuku, M. Kimathi, Nehad Ali Shah, and S. Saleem. Significance of Coriolis force, volume fraction, and heat source/sink on the dynamics of water conveying 47 nm alumina nanoparticles over a uniform surface. Chinese Journal of Physics, 2021. ISSN 0577-9073. https://doi.org/10.1016/j.cjph.2021.02.005

[3] R. K. Alhefthi, J. C. Umavathi, M. Inc, and A. S. Oke. Effects of radiative heat flux on MHD squeezing Newtonian flow between convectively heated parallel disks. Pramana, 97(4): 178, 2023.

[4] Huda Alsaud, Anthony R. Hassan, Mustafa Inc, Akeem B. Disu, Abayomi S. Oke, and Shahram Rezapour. Thermodynamic survey of a reactive MHD couple stress fluid through saturated porous substances with convective boundary conditions. Modern Physics Letters B, page 2450353, 2024.

[5] A. S. Oke. Coriolis effects on MHD flow of MEP fluid over a non-uniform surface in the presence of thermal radiation. International Communications in Heat and Mass Transfer, 129: 105695, December 2021. ISSN 0735-1933. https://doi.org/10.1016/j.icheatmasstransfer.2021.105695

[6] Rasheed Khan, Salman Zeb, Zakir Ullah, Muhammad Yousaf, and Inna Samuilik. Carreau fluid flow analysis with inclined magnetic field and melting heat transfer. Partial Differential Equations in Applied Mathematics, 13: 101030, March 2025. ISSN 2666-8181. https://doi.org/10.1016/j.padiff.2024.101030

[7] R. Leelavathi, Seethamahalakshmi Vyakaranam, T. S. Rao, Venkata Ramana Reddy Gurrampati, and Abayomi Samuel Oke. Mhd casson fluid flow in stagnation-point over an inclined porous surface. CFD Letters, 16(4): 69-84, 2024.

[8] T. Salahuddin, Saba Tariq, Mair Khan, Muhammad Awais, and M. Afzal. Electro-osmotic analysis of williamson fluid model with viscous dissipation and enthalpy. Results in Engineering, 25: 103635, March 2025. ISSN 2590-1230. https://doi.org/10.1016/j.rineng.2024.103635

[9] J. O. Ouru, W. N. Mutuku, and A. S. Oke. Buoyancy-Induced MHD Stagnation Point Flow of Wil-liamson Fluid with Thermal Radiation. Journal of Engineering Research and Reports, pages 9-18, 2020. https://doi.org/10.9734/jerr/2020/v11i417065

[10] Abayomi Samuel Oke, Belindar Atieno Juma, and Gurrampati Venkatta Ramana Reddy. Heat and mass transfer in MHD flow of SWCNT and graphene nanoparticles suspension in Casson fluid. ZAMM-Journal of Applied Mathematics and Mechanics/Zeitschrift für Angewandte Mathematik und Mechanik, page e202300106, 2024.

[11] Seethamahalakshmi Vyakaranam, Rekapalli Leelavathi, Tagallamudi Srinivasa Rao, Venkata Ramana Reddy Gurrampati, and Oke Abayomi Samuel. Soret-Dufour Mechanisms on Unsteady Boundary Layer Flow of Tangent Hyperbolic and Walters-B Nanoliquid. Journal of Advanced Re-search in Fluid Mechanics and Thermal Sciences, 108(1): 13-27, 2023.

[12] Abayomi S. Oke, Temitope Eyinla, and Belindar A. Juma. Effect of Coriolis force on modified Eyring Powell fluid flow. Journal of Engineering Research and Reports, 24(4): 26-34, 2023.

[13] Celestine Chepkemoi Rutto, Isaac Chepkwony, and Abayomi Samuel Oke. Numerical Comparison of Cu and Al_2O_3 Nanoparticles in an MHD Water-based Nanofluid. Journal of Engineering Research and Reports, 26(6): 139-146, 2024.

[14] R. V. Williamson. The Flow of Pseudoplastic Materials. Industrial & Engineering Chemistry, 21(11): 1108-1111, nov 1929. https://doi.org/10.1021/ie50239a035

[15] Mair Khan, T. Salahuddin, Muhammad Malik Yousaf, Farzana Khan, and Arif Hussain. Variable diffusion and conductivity change in 3D rotating Williamson fluid flow along with magnetic field and activation energy. International Journal of Numerical Methods for Heat & Fluid Flow, 30(5): 2467-2484, 2020. https://doi.org/10.1108/HFF-02-2019-0145

[16] Belindar A. Juma, Abayomi S. Oke, Winifred N. Mutuku, Afolabi G. Ariwayo, and Olum J. Ouru. Dynamics of Williamson fluid over an inclined surface subject to Coriolis and Lorentz forces. Engin-eering and Applied Science Letter, 5: 37-46, 2022. https://doi.org/10.30538/psrp-easl2022.0083

[17] T. A. Yusuf and F. Mabood. Slip effects and entropy generation on inclined MHD flow of Willi-amson fluid through a permeable wall with chemical reaction via DTM. Mathematical Modelling of Engineering Problems, 7(1): 1-9, 2020. https://doi.org/10.18280/mmep.070101

[18] Thadakamalla Srinivasulu and B. Shankar Goud. Effect of inclined magnetic field on flow, heat and mass transfer of Williamson nanofluid over a stretching sheet. Case Studies in Thermal Engineering, 23: 100819, 2021. ISSN 2214-157X. https://doi.org/10.1016/j.csite.2020.100819

[19] Yi-Xia Li, Mohammed Hamed Alshbool, M. Riaz Khan, Ilyas Khan, Yu-Pei Lv, and Alibek Issakhov. Heat and mass transfer in MHD Williamson nanofluid flow over an exponentially porous stretching surface. Case Studies in Thermal Engineering, page 100975, 2021. ISSN 2214-157X. https://doi.org/10.1016/j.csite.2021.100975

[20] Sakinah Idris, Anuar Jamaludin, Roslinda Nazar, and Ioan Pop. Joule heating and viscous dissipation impact on mhd-hybrid nanofluid flow over non-isothermal stretching/shrinking surface: Dual solution and stability analysis. Chinese Journal of Physics, December 2024. ISSN 0577-9073. https://doi.org/10.1016/j. cjph.2024.12.019

[21] Yongjie Xue, Yi Zhou, Jian Liu, Yue Xiao, and Teng Wang. Comparative analysis for pyrolysis of sewage sludge in tube reactor heated by electromagnetic induction and electrical resistance furnace. Waste Management, 120: 513-521, February 2021. ISSN 0956-053X. https://doi.org/10.1016/j.wasman.2020. 10.015

[22] O. K. Koriko, K. S. Adegbie, A. S. Oke, and I. L. Animasaun. Exploration of Coriolis force on motion of air over the upper horizontal surface of a paraboloid of revolution. Physica Scripta, 95(3): 035210, February 2020. ISSN 1402-4896. https://doi.org/10.1088/1402-4896/ab4c50

[23] O. K. Koriko, K. S. Adegbie, A. S. Oke, and I. L. Animasaun. Corrigendum: Exploration of Coriolis force on motion of air over the upper horizontal surface of a paraboloid of revolution. (2020 Phys. Scr. 95 035210). Physica Scripta, 95(8): 119501, October 2020. https://doi.org/10.1088/1402-4896/abc19e

[24] A. S. Oke, W. N. Mutuku, M. Kimathi, and I. L. Animasaun. Insight into the dynamics of non-Newtonian Casson fluid over a rotating non-uniform surface subject to Coriolis force. Nonlinear Engineering, pages 1-17, 2020. https://doi.org/10.1515/nleng-2020-0025

[25] Bagh Ali, N. Ameer Ahammad, Windarto, Abayomi S. Oke, Nehad Ali Shah, and Jae Dong Chung. Significance of Tiny Particles of Dust and TiO2 Subject to Lorentz Force: The Case of Non-Newtonian Dusty Rotating Fluid. Mathematics, 11(4): 877, 2023.

[26] Abayomi S. Oke, Winifred N. Mutuku, Mark Kimathi, and Isaac Lare Animasaun. Coriolis effects on MHD newtonian flow over a rotating non-uniform surface. Proceedings of the Institution of Mechan-ical Engineers, Part C: Journal of Mechanical Engineering Science, page 0954406220969730, 2020. https://doi.org/10.1177/0954406220969730

[27] Abayomi Samuel Oke. Heat and mass transfer in 3D MHD flow of EG-based ternary hybrid nanofluid over a rotating surface. Arabian Journal for Science and Engineering, 47(12): 16015-16031, 2022.

[28] Sujesh Areekara, A. S. Sabu, Alphonsa Mathew, and A. S. Oke. Transport phenomena in Darcy-Forchheimer flow over a rotating disk with magnetic field and multiple slip effects: modified Buon-giorno nanofluid model. Waves in Random and Complex Media, pages 1-20, 2023.

[29] Siva Reddy Sheri and Prasanthi Modugula. Heat and Mass Transfer Effects on Unsteady MHD Flow over an Inclined Porous Plate Embedded in Porous Medium with Soret-Dufour and Chemical Reac-tion. International Journal of Applied and Computational Mathematics, 3(2): 1289-1306, 2017. ISSN 2199-5796. https://doi.org/10.1007/s40819-016-0177-4

[30] A. S. Oke. Convergence of Differential Transform Method for Ordinary Differential Equations. Journal of Advances in Mathematics and Computer Science, 24(6): 1-17, 2017.

[31] Kamran Ahmed and Tanvir Akbar. Numerical investigation of magnetohydrodynamics Williamson nanofluid flow over an exponentially stretching surface. Advances in Mechanical Engineering, 13(5): 168781402110198, may 2021. https://doi.org/10.1177/16878140211019875